Diverse Climatic and Anthropogenic Impacts on Desertification in the Middle Reaches of Yarlung Zangbo River Catchment on the Tibetan Plateau

Qi Yu [1], **Xianyan Wang** [*1, 2], **Zhiyong Han** [1], **Xiaodong Miao** [3], **Huayu Lu** [1]

1. *School of Geography and Ocean Science, Nanjing University, Nanjing 210023, China*
2. *Key Laboratory of Tibetan Plateau Land Surface Processes and Ecological Conservation (Ministry of Education), Xining 810016, China*
3. *Shandong Provincial Key Laboratory of Water and Soil Conservation and Environmental Protection, School of Resource and Environmental Sciences, Linyi University, Linyi 276000, China*

Qi Yu: https://orcid.org/0000-0002-8323-6769; Xianyan Wang: https://orcid.org/0000-0002-8281-5734

ABSTRACT: The unique desertification processes occurring under the Alpine climate and ecosystem on the Tibetan Plateau could provide critical clues to the natural and anthropogenic impacts on desertification. This study used the Landsat data to investigate the spatial and temporal distribution of desertification from 1990 to 2020 in two areas (Shannan and Mainling), within the Yarlung Zangbo River Basin. The results show not only distinct spatial patterns but also various temporal changes of desertification. In Shannan, aeolian sand was distributed over wide areas from valley floor to mountain slope, while in Mainling, it is distributed sporadically at the footslope. The aeolian sandy land initially expanded before undergoing long-term shrinkage in Shannan. While in Mainling, it steadily expanded followed by a rapid decrease. These changes are attributed to both climate change and human activites. The increase in temperature causes desertification expansion in Shannan, while favorable climate conditions coupled with decreasing human activity promoted desertification reversal. However, both the expansion and shrinkage of desertification were sensitive to human activity in Mainling. This highlights the diverse responses of desertification to natural and anthropogenic impacts on different backgrounds of climatic and vegetation coverage. A threshold of climatic conditions may control the dominance factors in desertification, shifting from natural to anthropogenic elements.
KEY WORDS: desertification, reversal of desertification, human activities, climate change, remote sensing, Yarlung Zangbo River valley.

0 INTRODUCTION

Desertification can be defined as a major type of land degradation in arid and semiarid environments resulted from many factors such as climate change and human activities (Rasmussen et al., 2001). It is one of the most serious global eco-environmental challenges, and its consequences directly affect the sustainable development of the eco-environment and human society (Lyu et al., 2020; Reynolds et al., 2007). Desertification is a complex phenomenon, usually driven by multiple factors. Both climate change and human activities are driving factors for the occurrence, expansion and reversal of desertification (Xu and Lu, 2021; Moghaddam et al., 2018; Ajaj et al., 2017), but their relative contributions to desertification in different environments remain largely uncertain (Li et al., 2016a; Xu

et al., 2014). Understanding the dynamics of desertification and the mechanisms driving its changes could provide a basis for the formulation of control measures and better control the expansion of desertification in the future. As a result, monitoring the trend of desertification and understanding its feedback to climate change and human activities have become the focus of many studies.

China has some of the most widespread areas in the world with serious problems of desertification, especially in northern and northwestern China (Guo et al., 2014; Wang F et al., 2013; Wang T et al., 2002). In previous studies, most researches have attributed the rapid expansion of desertification in North China to human activities, such as population increase, economic growth, long-term overgrazing, and expansion of agricultural land in some areas (e.g., Wang et al., 2010; Liu and Diamond, 2005; Zhao et al., 2005). However, some researchers argue that temperature rise and reduction in precipitation are the primary factors leading to the occurrence and expansion of desertification (e. g., Wang et al., 2005; Hai et al., 2002). Recent studies have shown that climate change, as well as management policies (e.g., afforestation and grazing reduction), may have played

important roles in desertification restoration (e.g., Xu and Ding, 2018; Wang et al., 2013; Xu et al., 2009). Therefore, the extent to which climate change and human activities have led to desertification and regeneration in China remains a long-standing debate (Wang et al., 2013; Xu et al., 2009).

The unique atmospheric circulation patterns and the high altitude of the Tibetan Plateau have created a cold, dry, and fragile ecological environment that is highly vulnerable to desertification (Yang et al., 2020a; Yao and Zhu, 2006). Variations in wind and interannual fluctuations in precipitation affect vegetation growth in plain areas such as the Mu Us desert, in turn, influences the desertification process (e.g., Xu and Lu, 2021). While desertification on the Tibetan Plateau is attributable to rising temperature and the extensive thawing of permafrost, which result in the desiccation of surface soil and a reduction in vegetation cover (Xue et al., 2009). On the other hand, irrational human activities have created favorable conditions for aeolian desertification today. As the source of many river systems in Asia (Immerzeel et al., 2010), the expansion of desertification on the Tibetan Plateau not only affects the local eco-environment and economic development, but also affects the dynamics of the eco-environment of China and even that of entire Asia (Li et al., 2019; Dong et al., 2017). The development of desertification on the Tibetan Plateau could make the land with higher albedo, which would influence climate change on a regional scale (e.g., Dong et al., 2017). Therefore, monitoring desertification change processes and their mechanisms on the Tibetan Plateau is essential to better prediction of future environmental changes at regional scales.

The Yarlung Zangbo River Basin (YZRB) (Fig. 1), an area sensitive to the evolution of the eco-environment located at the southern edge of the Tibetan Plateau, has suffered severe desertification in the last couple of decades (Dong et al., 1999; Li et al.,

1997; Yang, 1984). Due to favorable conditions such as extensive sand sources, strong winds, and suitable deposition fields in the basin, aeolian landforms have developed extensively (Ling et al., 2020; Yang et al., 2020b). The middle reaches of the YZRB are the political, economic and social center of Tibet. In this region, the expansion of aeolian sandy lands has significant impact on agriculture, transportation and residents' health. Since 1990, many researchers have taken the changes in aeolian sandy land area as one of the indicators of land desertification development (e.g., Chang et al., 2006; Li et al., 1999; Liu et al., 1997). It was argued that the aeolian sandy lands show a discontinuous zonal distribution along the wide valley of the YZRB, and their area is constantly expanding, which may be the result of both climate warming (as the internal driving force) and irrational human activities (as the external driving force) (e.g., Liu et al., 2019; Zhou et al., 2014; Shen et al., 2012; Zhao et al., 2012).

However, most previous studies in the middle reaches of the YZRB mainly provide investigation results before 2010, and there is a lack of regional analysis of the driving factors of desertification. In addition, the previous studies were conducted at decadal intervals and lacked long-term time-series monitoring work. It is still not clear on the trend of desertification land in the past decade: whether it is reversing or expanding, and whether the regional differences in desertification are driven by climate or human factors. Here, we monitored the spatiotemporal variations in aeolian sandy lands in the middle part of the YZRB using the analysis of Landsat images from 1990 to 2020. Based on discussing the roles of climate change and human activities in aeolian desertification, we aim to provide the basis for an improved understanding of climate change and anthropogenic factors on desertification under different eco-environments and economic development backgrounds.
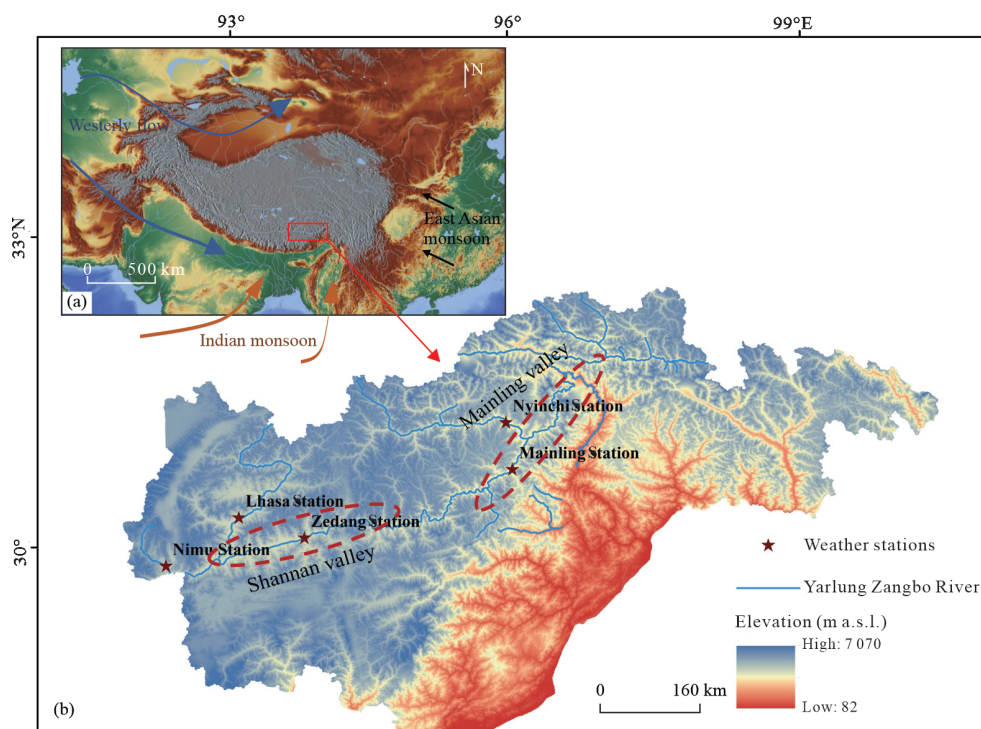

Figure 1. (a) Geographical location of the study area (modified from Yao et al., 2017). (b) Topographic map of the study area.

1 STUDY AREA

The Yarlung Zangbo River, stretching across the southern part of the Tibetan Plateau from west to east, originates from Jemaangzong Glacier in the northern part of the Himalayas Mountains, with a drainage area of 2.4×10^5 km² in China and an average altitude of over 4 000 m (Fig. 1; Shi et al., 2018; Yao et al., 2010). The YZRB consists of alternating sections of wide valleys and gorges. The wide valley sections mainly exhibit anastomosing channels with gentle bed gradients and thick alluvial deposits (Wang et al., 2016). During the dry season, a large amount of river alluvium is exposed, which provides abundant sand sources for the regional aeolian activities. Meanwhile, alluvial plains and terraces in the wide valleys provide ideal deposition fields, coupled with dry-and-cold, windy climate conditions. All of them make the aeolian sandy lands widely distributed in this region (Fig. 1; Li et al., 1997). In contrast, single, straight, and deeply incised meandering channels are developed in gorge sections with a steep gradient and rock channel bed (Wang et al., 2016).

The YZRB is divided into four wide valley sections from east to west, namely the Maquan River wide valley, Shigatse wide valley, Shannan wide valley and Mainling wide valley (Fig. 1b). In this study, the Shannan valley and Mainling valley in the middle reaches of the YZRB, which have intensive human activities and different eco-environments, are selected as the main research areas. The Shannan valley has a semiarid alpine climate (Shen and Li, 2012). The mean annual temperature is approximately 6–8 ℃, and the mean annual precipitation is approximately 400 mm (Ling et al., 2019), falling mainly in July and August with distinct dry and wet seasons (Fig. 2a). The Mainling valley is mainly affected by a sub-humid monsoon climate with better vegetation cover than the Shannan (Fig. 2b). The mean annual temperature is about 8.2 ℃ in the Mainling valley, with an annual precipitation of 641 mm, most of which is concentrated from June to September (Zhou et al., 2014). Affected by local topography and climate, both valleys exhibit strong southwest winds, of which in spring and winter are mainly controlled by west winds (Fig. 1a; Ling et al., 2019; Shen et al., 2012).

2 MATERIALS AND METHODS
2.1 Classification System for Aeolian Sandy Land

In the middle reaches of the YZRB, desertification is the leading form of land degradation. The destruction of the natural vegetation cover contributes to severe wind erosion, accompanied by the development of discontinuous zonal and patchy aeolian sandy land, and they provide good visual indicators of the dynamics of desertification. We use the vegetation cover, surface soil composition, and aeolian landforms inferred from Landsat images as indices of the status of aeolian sandy land. Based on the classification criteria proposed in previous studies (Shen and Li, 2012; Li et al., 1997; Zhu et al., 1994; Yang, 1984), interpretation of Landsat images and field survey data, we classified aeolian sandy land into five categories: fixed sand land, semi-fixed sand land, mobile sand land, bare sandy gravel land, and semi-exposed sandy gravel land (Table 1, Fig. 3). Among them, fixed sand land, semi-fixed sand land, and mobile sand land belong to wind-deposited sand land, while bare and semi-exposed sandy gravel land belong to wind-eroded sand land.

2.2 Landsat Images Data and Data Processing

Landsat images have been widely used to monitor the temporal and spatial dynamics of desertification for a long time because of their extensive coverage, long-term continuous time series and accessibility (Wang et al., 2018; Jiang et al., 2013). The Landsat TM/ETM and OLI data collected in this study included 39 scenes (three scenes at each period with orbital parameters of 135/040, 136/040, and 137/040) for every two or three years (1990, 1993, 1995, 1997, 2001, 2003, 2006, 2009, 2011, 2013, 2015, 2017 and 2020). The spatial resolution of these data is 30 m, and the cloud cover of each scene is less than 8%. All remote sensing images were downloaded from the Geospatial Data Cloud (http://www.gscloud.cn/). Images were obtained for periods from November to January in this study, depending on precipitation in these months being sparse and there being little cloud cover.

All images were preprocessed by radiation correction, geometric correction, and atmospheric correction. We preprocessed the selected images using version 5.3 of ENVI Imagine software (Deng, 2010). Using 1 : 100 000 topographic maps, the 1990 TM images were geometrically corrected and 50 ground control points (GCPs) were selected for each image to ensure the corrected accuracy in the range of one pixel. We then used the calibrated images as references to repeat the correction of the other 12 sets of images (Guo et al., 2021). To acquire 13 sets of Landsat images for the valleys with a consistent tone, geometrically corrected images were obtained by
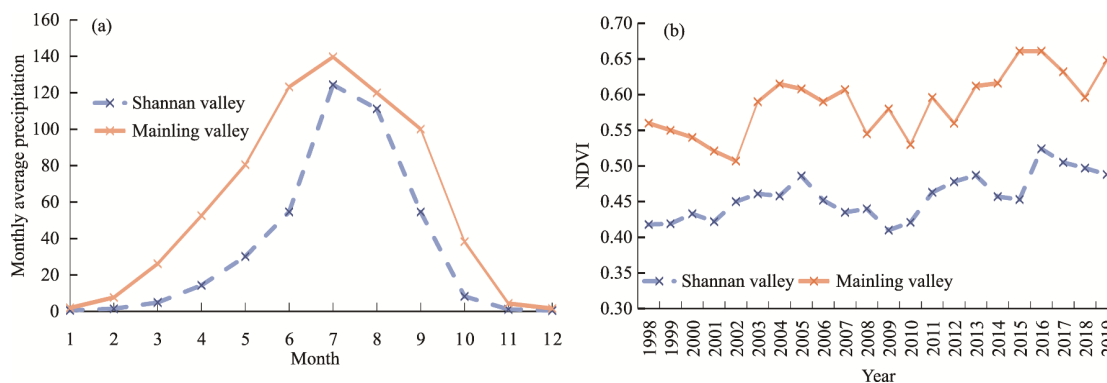

Figure 2. (a) Variations of average monthly precipitation; (b) NDVI (Normalized Vegetation Index) of the Shannan valley and Mainling valley in the last 20 years.

Figure 3. Classifications of aeolian sandy land in the middle reaches of Yarlung Zangbo River basin.

Table 1   Classification and interpretation signs of aeolian sandy land types

Type	Proportion of the area covered by gravels	Vegetation cover	Surface feature	Tone and texture of Landsat images	Typical Landsat TM/ETM/ OLI image (combination of bands 4, 3, and 2)
Mobile sand land	<10%	<10%	Sand dunes are widely distributed, including flat sand, crescent dunes, dune chains and composite dunes	Almost no vegetation exists. Tone shows a bright white color, with clear mobile dune shape. There is wavy texture feature	
Semi-fixed sand land	<10%	20%–40%	Sand dunes are scattered, with a small amount of moving sand, forming a sandy grassland landscape	Brightness is low due to sparse sand surface vegetation, light pink color, with rough surface textures	
Fixed sand land	<10%	>50%	Sand dunes are scattered or sparsely distributed with fixed flat sand and dune, grassland and sandy grassland landscapes	Tone shows a dark color due to dense vegetation the sand surface, with rough surface textures	
Semi-exposed sandy gravel land	>10%	<10%	Erosion exposes rough gravel and sparse dunes, with small coppice dunes	Tone is similar to that of fixed sandy land, but darker due to the higher gravel content, with a rough surface texture	
Bare sandy gravel land	>10%	15%–40%	Coarse sands and gravel, with sparse dunes or sheets of gravel and sand, exposing a gobi-type landscape	Tone is bright white, with a smooth surface texture	

means of an image-to-image matching method. In 2020 and 2021, we conducted field investigations in the middle reaches of the YZRB, including recording the location, distribution characteristics, surface texture, vegetation coverage and other characteristics of different types of sandy lands. Subsequently, these images were compared, and the interpretation marks were established. The sandy land surface has a very high albedo compared to other objects and can be clearly distinguished from other surrounding land types (Table 1). With ENVI5.3 and ArcGIS10.2, sandy lands were interpreted by means of a

visually interactive interpretation method from false color images synthesized from the 4/3/2 band of Landsat TM/ETM/ OLI data. In addition, by selecting 60 random points with uniform spatial distribution and including all types of sandy lands, the environmental information and landscape photos of random points were recorded in the field. These verification points and interpretation results were compared and analyzed to evaluate the accuracy of the interpretation results. The accuracy evaluation and Kappa coefficient calculation of the interpretation results showed that the classification accuracy of each image was above 92%, and the Kappa coefficient was above 0.88. The results indicate that this classification method performed well to distinguish sandy lands.

2.3 Climatic and Anthropogenic Factors

Climate change and human activities are two major factors that drive desertification (Mirzabaev et al., 2019; Moghaddam et al., 2018; Wang et al., 2009). Among the climate factors, temperature, rainfall, and wind velocity played crucial roles in desertification (Na et al., 2019). To examine their effects, we collected monthly climatic data from five weather stations in the Shannan valley and Mainling valley (Fig. 1b) from 1990 to 2020. All data are provided by the National Meteorological Science Data Center (http://data.cma.cn/).

In the middle reach of the YZRB, the desertification process was closely associated with unsustainable land use, such as overgrazing and over-reclamation of arable land. The increasing population has put heavy pressure on the region's fragile ecological environment. Consequently, among the anthropogenic factors, population, arable land area and livestock numbers were used as indices of the intensity of human activities, which contributed greatly to desertification (Shen et al., 2015; Li et al., 2010). To examine their effects, we collected the above socio-economic data of Shannan and Nyinchi cities, which occupy the Shannan valley and Mainling valley, respectively, during the 1990–2019 period from the Tibetan Statistical Yearbook.

We analyzed the long-term changes in climate (air temperature, annual precipitation, and mean annual wind velocity) and human activity (population, arable land area and livestock numbers) using linear regression. After establishing the regression equation, the goodness-of-fit (R^2) test of the regression equation and the significance test of the regression coefficient (t-test) were carried out. When R^2 is closer to 1, the fitting degree of the regression equation is better; in contrast, when R^2 is closer to 0, the fitting degree is worse. The statistical analysis of the trend calculation results was performed using the t-test at a significance level of 10% ($P < 0.1$). The formula of the linear regression model is as follows

$$y = \beta_0 + \beta_1 x + \varepsilon$$

where, y represents the meteorological factor or socio-economic indicator, x refers to the annual time series, β_0 and β_1 are coefficients, and ε is the residual of the fitting.

To analyze the closeness of the correlation between affecting factors and changes in the aeolian sandy land area, we conducted a correlation analysis on the sandy land area interpreted since 1990 and different driving factors. In this study, the Pearson correlation coefficient R was used to measure the degree of

closeness between the two variables (Xue, 2014). The formula is as follows

$$R = \frac{\sum_{i=1}^{N}(X_n - \bar{X})(Y_n - \bar{Y})}{\sqrt{\sum_{i=1}^{N}(X_n - \bar{X})^2 \sum_{i=1}^{N}(Y_n - \bar{Y})^2}}$$

where $\bar{X}$ and $\bar{Y}$ are the average values of the data. The R values range from -1 to 1. The closer the absolute value of the correlation coefficient is to 1, the stronger the correlation between Y and X. In contrast, if R equals 0, there is no correlation between the two variables. Generally, if $|R| \geq 0.8$, it can be regarded as a high correlation; if $0.5 \leq |R| < 0.8$, there is a moderate correlation; and if $0.3 \leq |R| < 0.5$, it can be regarded as a weak correlation. $|R| < 0.3$, indicating that the correlation between the two variables is extremely weak, which can be regarded as a nonlinear correlation (Xue et al., 2014).

3 RESULTS
3.1 Spatial Distribution of Aeolian Sandy Land

The aeolian sandy lands in the middle reaches of the YZRB present a discontinuous zonal and patchy distribution along the wide valleys. Aeolian sand landforms in the Shannan valley were prominent from the valley floor extending to the mountain slope, especially on the north bank (Fig. 4a). Within wind-deposited sand land, mobile sand lands were mostly distributed around flood-plains, and on alluvial-pluvial fans and hill slopes. Semi-fixed sand lands and fixed sand lands were primarily distributed on river terraces, alluvial-pluvial fans and flood plains. Bare and semi-exposed sandy gravel lands were mainly distributed in seasonally dry riverbeds, middle and upper alluvial-pluvial fans (Fig. 4a). Each type of aeolian sandy land was dispersedly distributed along the foot of hill slopes and flood-plains in the Mainling valley (Fig. 4b).

3.2 Temporal Changes of Aeolian Sandy Land

Generally, the area of sandy lands in the two wide valleys first increased and then decreased during the 1990–2020 period (Fig. 5). Sandy lands in the Shannan valley increased by 78.14 km² during the 1990–2009 period, with an average annual increase rate of 3.91 km²/yr. Among them, the area of sandy lands increased the fastest, with a total rise of 58.64 km² and an annual increase rate of 5.33 km²/yr from 1990 to 2001. From 2009 to 2020, sandy lands decreased by 80.12 km², which equalled an annual decrease of 6.68 km², suggesting a reversal trend of desertification (Table S1). From 1990 to 2015, the area of sandy lands in the Mainling valley increased by 47.28 km², whereas in 2015–2020, the area decreased by 27.24 km², indicating an annual decrease rate of 5.45 km²/yr in the last five years (Table S1).

3.3 Changes of Diferent Types of Aeolian Sandy Land

In total, there were 358.83 km² of sandy lands in the Shannan valley in 2020. The areas of wind deposition and wind erosion of sandy lands were 302.52 and 56.31 km², accounting for 84.31% and 15.69% of the total aeolian sandy land, respectively. In the same year, 97.92 km² of sandy lands were covered in the Mainling valley. Among them, the areas of wind deposition and wind erosion of aeolian sandy lands were 88.82 and 9.10
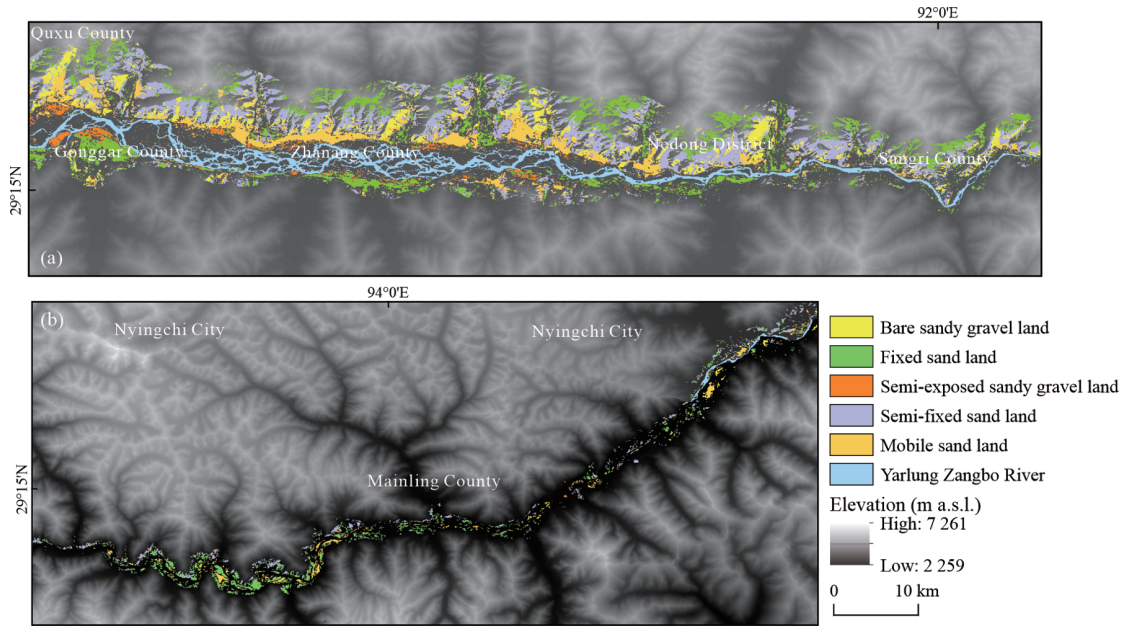
Figure 4. Distribution of classified major aeolian sandy lands in the Shannan and Mainling areas in 2020.
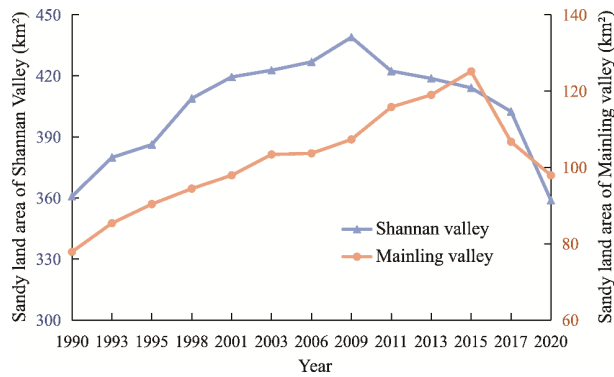

Figure 5. The area changes of aeolian sandy land in the Shannan valley and Mainling valley from 1990 to 2020.

km², accounting for 90.71% and 9.29% of the total sandy land, respectively (Table S2).

In the past 30 years in the Shannan valley, semi-fixed sand land occupied the largest area, followed by fixed sand and mobile sand land. In the more erosional sand land, the area proportion of the bare sandy gravel land and the semi-exposed sandy gravel land had little difference. During the expansion stage of the sandy land area, the fixed sandy land area increased the most, while in the desertification reversal stage, the area of semi-fixed sandy land and mobile sand land decreased the fastest (Fig. S1a). In the Mainling valley, fixed sandy land accounts for the largest proportion, followed by semi-fixed sandy land and mobile sandy land. The two types of wind-eroded sandy land account for a relatively small area. In the period of increasing sandy land area, the semi-fixed sand land grew the fastest, while during the desertification reversal stage, the area of fixed and mobile sand land decreased rapidly (Fig. S1b).

3.4 Correlation between Aeolian Land and Climatic and Anthropogenic Factors

The correlation analysis showed that the changes in aeoli-an sandy land area were positively correlated with the temperature in both valleys. Especially in the Shannan valley, the correlation coefficient between the aeolian sandy land area and air temperature is the highest (Fig. 6a). The changes in aeolian sandy land area of the two valleys are negatively correlated with precipitation and wind velocity. In terms of anthropogenic impacts, there is a close linear relationship between the area of aeolian sandy land and one of the indirect indices of the intensity of human activity, the population (Fig. 6). In particular, the changes in aeolian sandy land in the Mainling valley are closely related to the population and the number of livestock (Fig. 6b).

4 DISCUSSION
4.1 Cause of the Different Spatial Distribution Patterns of Sandy Land in Different Areas

The difference in the spatial distribution of aeolian sandy land in the middle reaches of the YZRB is mainly related to topography and climatic factors. The width of the Shannan valley is much larger than that of the Mainling valley, and the wider valley may provide favorable topographic conditions for the accumulation of aeolian sand. In addition, the wider valley leads to generally developed braided and anastomosing channels in the Shannan valley (Fig. 4a). During the dry season, the channel bars are exposed to a large area, which provides abundant sand source for aeolian activities. As a result, the aeolian sandy land here spreads widely on the valley floor and extensively extended into the mountain slope. On the contrary, the valley in Mainling is relatively narrow with meandering channels, where aeolian sandy lands are distributed in discontinuous patches along the foot of the valley slope (Fig. 4b). The semiarid climate in the Shannan valley has the average precipitation obviously less than that in the Mainling valley. This difference in climate (Fig. 2a) results in different vegetation covers, which may protect the surface from wind deflation and help stabilize sand dunes. NDVI (Normalized Vegetation Index) values in these two areas (Fig. 2b), show that vegetation
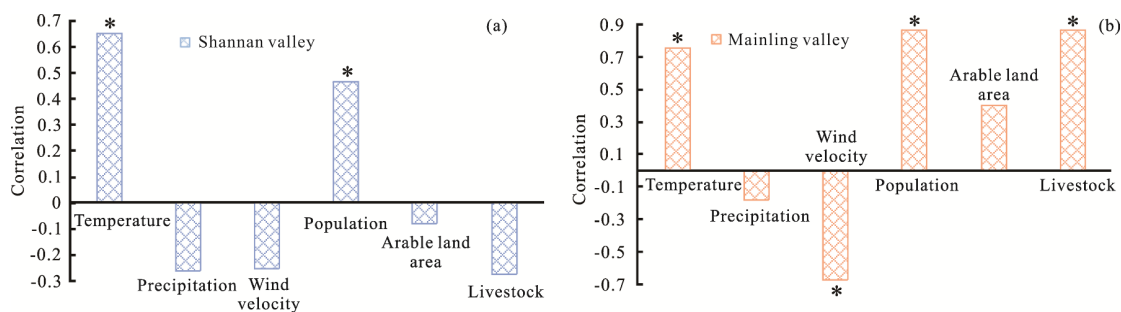
Figure 6. The correlation between the area of aeolian sandy land and the potential impact factors (* indicates a significant correlation at the $P < 0.05$ level).

coverage in Mainling valley is significantly higher, and the earth's surface is more stable than that in the Shannan valley. Hence, compared to the Mainling area, the Shannan area with the drier climate and lower vegetation coverage, larger flat areas, and specific river patterns (i.e., braided and anastomosed stream), resulted in a more extensive distribution of aeolian sandy land in the last 30 years (Figs. 4 and 6).

4.2 Diverse Response of Aeolian Desertification to Climatic and Anthropogenic Impacts

With variability in time and space, desertification is a complex environmental process affected by climate change and human activities (Mirzabaev et al., 2019). They have both accelerative and inhibitory effects. Our studies show that the driving factors of desertification have regional differences in the middle reaches of the YZRB. The semiarid Shannan valley has less precipitation and a fragile ecological environment, while the sub-humid Mainling valley has a better vegetation coverage. Due to this difference, the semi-fixed sandy land and mobile sandy land are mainly distributed in the Shannan valley, while the fixed sandy land occupies the largest area in the Mainling valley (Fig. 4).

Climate mainly affects desertification via temperature, precipitation and wind velocity (Na et al., 2019; Wang et al., 2009). The warming and decrease in precipitation may reduce soil water availability, soil fertility and vegetation coverage. Coupled with the increase in wind velocity, they could result in strong deflation, transportation and deposition of sandy materials. This is conducive to the expansion of aeolian sandy land in a dry environment (e.g., Zeng et al., 2021; Huang et al., 2020). From 1990 to 2010, the annual mean temperature in the Shannan valley increased significantly, with a rising rate of 0.06 °C/year (Fig. S2a). The annual precipitation in this valley showed a larger fluctuation, exhibiting a decreasing trend in general (Fig. S2b). The combination of rising temperatures and declining precipitation led to the expansion of the aeolian sand land during this period. The expansion of aeolian sandy land could be mainly promoted by the high annual mean temperature and dry environment (Fig. 6a). During the 2010–2020 period, the annual mean temperature showed a decreasing trend, while the annual precipitation increased significantly (Fig. S2b), which could be conducive to a wet climate and the suppression of desertification (Fig. 5).

During the whole period, the annual mean temperature in the Mainling valley showed an increasing trend (Fig. S2a), and the precipitation fluctuated and generally declined, especially after 2015 (Fig. S2b). This trend of climate change should be conducive to the expansion of aeolian sandy land. However, the area of aeolian sandy land continuously decreased after 2015, when the wind velocity increase should reinforce aeolian desertification (Fig. 5). This indicated that instead of climate factors as the causes of the desertification reversal in the Mainling valley, anthropogenic factors can be more important. In fact, the population and the quantity of livestock, which represent intensity of human activity, might be the major factors driving the variations in the area of aeolian sandy land (Fig. 6). In addition, the annual mean wind velocity in both valleys exhibited a distinct trend that decreased first and then increased (Fig. S2c). Thus, the variation trend of wind speed is negatively correlated with changes in areas of aeolian land in both valleys, indicating that wind speed should not be the dominant factor, controlling the expansion and shrinkage of aeolian sandy land here.

Irrational human activities, such as the expansion of arable land and overgrazing, may increase pressure on land resources from population growth and lead to land degradation and subsequent desertification (e.g., Xu and Lu, 2021; Moghaddam et al., 2018; Zhao et al., 2005). However, active human measures can prevent and control desertification, including fencing pastures to protect natural vegetation from overgrazing and planting shelter forest systems, which are beneficial to improve soil fertility and mitigate desertification (e. g., Xu and Ding, 2018; Wang et al., 2013; Xu et al., 2009). Since the 1960s, the economy of the Tibetan Plateau has developed rapidly, and the increasing population has put heavy pressure on the region's natural resources and fragile eco-environment. At the same time, the number of livestock and the area under cultivation have also increased (Fig. S3; Li et al., 2016b).

From 1990 to 2020, the total population of the study area increased. The population of Shannan increased from 283 000 in 1990 to 382 600 in 2019, with an annual population growth rate of 10‰ (Fig. S3a), which may promote the expansion of aeolian sandy land. The number of livestock here showed a decreasing trend, with a decline of 141 400 in the 1990–2010 period and 711 100 in the 2010–2019 period, with an even faster reduction (Fig. S3c). The number of livestock, arable land area and comprehensive human activity intensity index in Shannan decreased from 1990 to 2010 (Figs. S3b and 7), which should be conducive to the suppression of desertification. However, the areas of aeolian sandy land still increased during this period, indicating that rather than human activities, natural factors such as climate change was the dominant factor of desertification expansion during this period (Fig. 7).
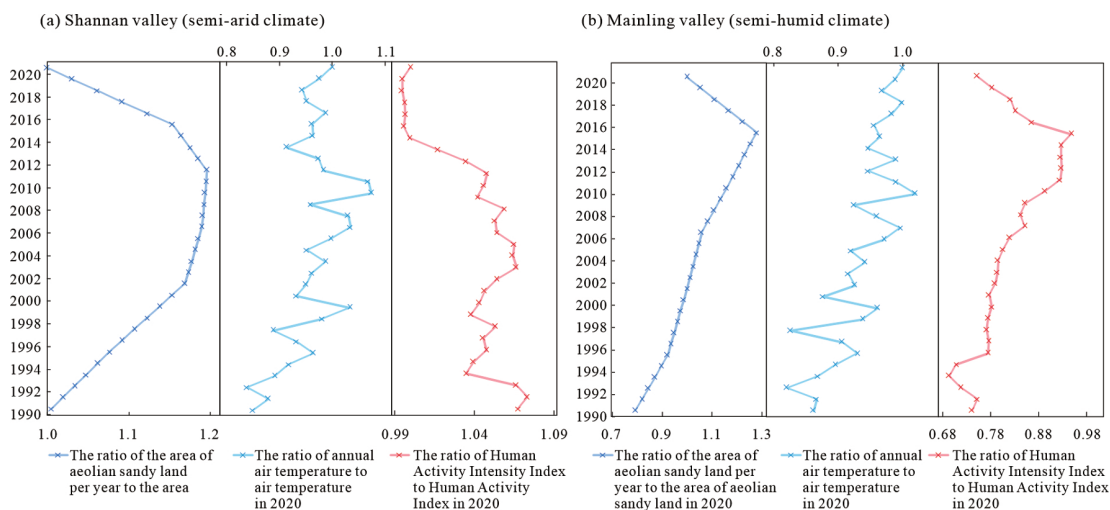
Figure 7. Variations in areas of aeolian sandy land, temperature, and the relative intensity of human activities in the (a) Shannan valley and (b) Mainling valley during 1990–2020. All indicators are standardized, and the intensity of human activities is calculated by the standardized results of population, arable land and livestock (weighted by the correlation coefficient).

The population of Nyinchi City in the Mainling valley increased rapidly from 1990 to 2019 by 108 900 people, with an annual population growth rate of 20‰ (Fig. S3a). The cultivated land area also showed an increasing trend, with a total rise of 3.68×10^3 ha in the past 30 years (Fig. S3b). The number of livestock and the comprehensive human activity intensity index exhibited a steady increase from 1990 to 2015 (Figs. S3c and 7), which should be conducive to the growth of the aeolian sandy land in the Mainling valley. In contrast, after 2015, the number of livestock and the comprehensive human activity intensity index showed a downward trend (Fig. 7), which may promote the reversal of desertification. The control of anthropogenic factors on the acceleration and reversal of desertification in the Mainling valley is somewhat similar to previously reported results in southern Tibet (Li et al., 2016b). It has been reported that unreasonable anthropogenic activities in economically developed southern Tibet, such as the increase in the number of livestock and excessive woodcutting have caused serious damage to natural vegetation and grassland soil, resulting in an area increase of bare land and the aggravation of desertification (Shen et al., 2015, 2012; Li et al., 2010; Dong et al., 1999). Since 1990, national and local governments have carried out a series of ecological restoration projects in Tibet, such as "Desertification Prevention and Control Engineering in the Valley of the Yarlung Zangbo River and the Shiquanhe Basin", "The Grain for Green Project", and "Construction of a National Ecological Security Barrier to Protect the Tibetan Plateau" (Li J C et al., 2020; Li Q et al., 2016b; Cheng et al., 2012). These projects (e.g., natural grassland protection and artificial afforestation) might have greatly increased the area of shelter forest in Shannan and Mainling, which might have promoted the restoration of a higher vegetation cover and improved soil fertility, thus mitigating desertification.

In conclusion, changes in aeolian sandy land in the last 30 years in both regions with distinct differences in climate and eco-environment have different responses to climate change and human activities (Fig. 7). The semiarid Shannan valley, with a relatively fragile ecosystem, was highly sensitive to climate change. Temperature fluctuations led to the expansion of aeolian sandy land from 1990 to 2010 (Fig. 7a), which is consistent with previous arguments that rising temperatures could be the dominant climate factor in desertification on the Tibetan Plateau (Yang et al., 2010; Xue et al., 2009). Rising temperatures will prolong the thawing period, thereby increasing the thickness of the active layer above the permafrost, which would subsequently lead to increased evaporation, desiccation of the surface soil and a reduction in vegetation cover (Cheng et al., 2012). Our results show that beneficial climate and large-scale ecological restoration projects have contributed to the reversal of desertification in the past ten years (Fig. 7a). In the future, a warmer and wetter climate may promote the growth of grassland (Cong et al., 2017) and alleviate the desertification. In the Mainling valley, the climate is more humid with higher vegetation coverage than in the Shannan valley. In the last 30 years, the dominant factors controlling desertification here have been related to human activities (Fig. 7b). Irrational human activities along with warming and drying of the climate have facilitated the expansion of aeolian sandy land, while artificial ecological restoration might lead to the reversal of the aeolian desertification in the past five years in Mainling area (Fig. 7b).

Based on the analysis of the driving factors of aeolian sand in the middle valley of the YZRB and previous studies on desertification on the Tibetan Plateau, it is shown that the effects of climatic and anthropogenic factors on aeolian sand desertification are significantly different from those on dry land in northern China. First, compared to northern China (Xu et al., 2014; Wang et al., 2002), the proportion of human factors in desertification on the Tibetan Plateau is obviously reduced. Second, among the climatic factors, temperature is the predominant factor of desertification on the Tibetan Plateau, while precipitation and wind velocity might have little influence on it. In addition, overgrazing could be the main anthropogenic factor of desertification on the Tibetan Plateau, but the destructive effect of over-reclamation might not be as important as in northern China. Compared with the desertification areas in northern China, the Tibetan Plateau region is recharged by snowmelt in

addition to precipitation, thus the fluctuation of precipitation might be relatively less restrictive to vegetation. In addition, the local landform within the plateau is complex, and the wind direction is complicated and variable due to the mountain blockage. The complex wind direction within the valley affects the distribution of sandy land, while the dispersing wind may make the effect of wind speed less obvious. In the plateau area, there are widely distributed bare and fragile land surfaces, and here the effect of relatively small artificial reclamation could be not significant on the desertification. This might indicate diverse responses of aeolian desertification to natural (e. g., climate) and anthropogenic impacts on different backgrounds of climatic and vegetation coverage. A threshold of climatic and ecological conditions could control the dominant factor in desertification from natural to anthropogenic elements. For example, the dominant factor in aeolian desertification is the intensity of human activity in Mainling under sub-humid environment, while it is climatic change in Shannan under semiarid environment on the Tibetan Plateau.

5 CONCLUSIONS

It shows that in the Shannan valley, the aeolian sandy land is distributed continuously, widely extending from the valley floor to the mountain slope, where the climate is dry and vegetation coverage is low, in the last 30 years. In contrast, it is distributed as scattered small patches at the foot of the valley side in the Mainling valley, where the climate is sub-humid with higher vegetation coverage. This disparity in the spatial distribution of desertification is related to different climates and vegetation coverage, along with morphological features such as river patterns and valley width.

Remote sensing and correlation analysis show that from 1990 to 2009, the area of aeolian sandy land in the Shannan valley increased as a result of increasing temperature, followed by a reversal of desertification from 2009–2020, under the condition of a beneficial climate along with ecological restoration projects. In the Mainling valley, irrational human activities along with warming and drying of the climate facilitated the expansion of the sandy land from 1990 to 2015, followed by shrinkage of aeolian sandy land as a result of artificial ecological restoration in the last five years.

In conclusion, the Shannan valley has a semiarid climate and fragile ecosystem and was highly sensitive to natural change of climate in the last 30 years, while anthropogenic factors controlled the process of desertification in the Mainling valley under conditions of a sub-humid climate and with relatively high vegetation coverage. This result shows diverse responses of desertification to natural and anthropogenic factors under different backgrounds of climate and vegetation coverage, even within the same catchment on the Tibetan Plateau. The extending records of desertification and more investigations into its specific responses to diverse natural and anthropogenic factors in different contexts could deepen our understanding on interlinked climatic and anthropogenic impacts on desertification.

Electronic Supplementary Materials: Supplementary materials (ESM Figs. S1–S3 and Tables S1–S2) are available in the online version of this article athttps://doi.org/10.1007/s12583-022-1658-5.

Conflict of Interest

The authors declare that they have no conflict of interest.

REFERENCES CITED

Ajaj, Q. M., Pradhan, B., Noori, A. M., et al., 2017. Spatial Monitoring of Desertification Extent in Western Iraq Using Landsat Images and GIS. *Land Degradation & Development*, 28(8): 2418–2431. https://doi.org/10.1002/ldr.2775

Chang, C. P., Zhou, X. R., Zhang, C. L., et al., 2006. The Characteristics and Distribution of the Source Area of Aeolian Sand in the Valley of Lhasa River's Lower Reaches, Tibet, China. *Mountain Research*, 24(4): 489–497. https://doi.org/10.1109/igarss.2006.791

Cheng, W. M., Zhao, S. M., Zhou, C. H., et al., 2012. Simulation of the Decadal Permafrost Distribution on the Qinghai-Tibet Plateau (China) over the Past 50 Years. *Permafrost and Periglacial Processes*, 23(4): 292–300. https://doi.org/10.1002/ppp.1758

Cong, N., Shen, M. G., Yang, W., et al., 2017. Varying Responses of Vegetation Activity to Climate Changes on the Tibetan Plateau Grassland. *International Journal of Biometeorology*, 61(8): 1433–1444. https://doi.org/10.1007/s00484-017-1321-5

Deng, S. B., 2010. ENVI Remote Sensing Image Processing Method. Science Press, Beijing. 54–164 (in Chinese)

Dong, Y. X., Li, S., Dong, G. R., 1999. Present Status and Cause of Land Desertification in the Yarlung Zangbo River Basin. *Chinese Geographical Science*, 9(3): 228–235. https://doi.org/10.1007/s11769-999-0048-6

Dong, Z. B., Hu, G. Y., Qian, G. Q., et al., 2017. High-Altitude Aeolian Research on the Tibetan Plateau. *Reviews of Geophysics*, 55(4): 864–901. https://doi.org/10.1002/2017rg000585

Guo, Y., Song, Z. Z., Ma, L., et al., 2021. Class-Wise Feature Alignment Based Transfer Network for Multi-Temporal Remote Sensing Image Classification. *Earth Science*, 46(10): 3730–3739. https://doi.org/10.3799/dqkx.2020.347 (in Chinese with English Abstract)

Guo, Z. L., Huang, N., Dong, Z. B., et al., 2014. Wind Erosion Induced Soil Degradation in Northern China: Status, Measures and Perspective. *Sustainability*, 6(12): 8951–8966. https://doi.org/10.3390/su6128951

Hai, C. X., Ma, L., Wang, X. M., et al., 2002. Main Factors Analysis about Soil Desertification in Typical Section of Interlock Area of Farming and Pasturing: The Case of Zhangbei County——Bashang Area of Hebei Province. *Geographical Research*, 21(5): 543–550 (in Chinese with English Abstract)

Huang, J. P., Zhang, G. L., Zhang, Y. T., et al., 2020. Global Desertification Vulnerability to Climate Change and Human Activities. *Land Degradation & Development*, 31(11): 1380–1391. https://doi.org/10.1002/ldr.3556

Immerzeel, W. W., van Beek, L. P. H., Bierkens, M. F. P., 2010. Climate Change will Affect the Asian Water Towers. *Science*, 328(5984): 1382–

1385. https://doi.org/10.1126/science.1183188

Jiang, G. Z., Han, B., Gao, Y. B., et al., 2013. Review of 40-Year Earth Observation with Landsat Series and Prospects of LDCM. *National Remote Sensing Bulletin*, 17(5): 1033–1048. https://doi.org/10.11834/jrs.20132296

Li, J. C., Wang, Y., Zhang, L. S., et al., 2019. Aeolian Desertification in China's Northeastern Tibetan Plateau: Understanding the Present through the Past. *CATENA*, 172: 764–769. https://doi.org/10.1016/j.catena.2018.09.039

Li, J. C., Yao, Q., Zhou, N., et al., 2020. Modern Aeolian Desertification on the Tibetan Plateau under Climate Change. *Land Degradation & Development*, 32(5): 1908–1916. https://doi.org/10.1002/ldr.3862

Li, Q., Zhang, C. L., Shen, Y. P., et al., 2016a. Quantitative Assessment of the Relative Roles of Climate Change and Human Activities in Desertification Processes on the Qinghai-Tibet Plateau Based on Net Primary Productivity. *CATENA*, 147: 789–796. https://doi.org/10.1016/j.catena.2016.09.005

Li, Q., Zhang, C. L., Shen, Y. P., et al., 2016b. Developing Trend of Aeolian Desertification in China's Tibet Autonomous Region from 1977 to 2010. *Environmental Earth Sciences*, 75(10): 1–12. https://doi.org/10.1007/s12665-016-5709-z

Li, S., Dong, G., Shen, J. Y., et al., 1999. Formation Mechanism and Development Pattern of Aeolian Sand Landform in Yarlung Zangbo River Valley. *Science in China Series D*: *Earth Sciences*, 42(3): 272–284. https://doi.org/10.1007/bf02878964

Li, S., Wang, Y., Ha, S., et al., 1997. Classification and Development of Aeolian Sand Landform in the Yarlung Zangbo Valley. *Journal of Desert Research*, 17(4): 342–350 (in Chinese with English Abstract)

Li, S., Yang, P., Dong, Y. X., et al., 2010. Land Desertification and Its Control in Tibet. Science Press, Beijing. 77–157 (in Chinese)

Ling, Z. Y., Jin, J. H., Wu, D., et al., 2019. Aeolian Sediments and Their Paleoenvironmental Implication in the Yarlung Zangbo Catchment (Southern Tibet, China) since MIS3. *Acta Geographica Sinica*, 74(11): 2385–2400. https://doi.org/10.11821/dlxb201911014 (in Chinese with English Abstract)

Ling, Z. Y., Yang, S. L., Wang, X., et al., 2020. Spatial-Temporal Differentiation of Eolian Sediments in the Yarlung Tsangpo Catchment, Tibetan Plateau, and Response to Global Climate Change since the Last Glaciation. *Geomorphology*, 357: 107104. https://doi.org/10.1016/j.geomorph.2020.107104

Liu, J. G., Diamond, J., 2005. China's Environment in a Globalizing World. *Nature*, 435(7046): 1179–1186. https://doi.org/10.1038/4351179a

Liu, L. Y., Liu, Z. M., Wang, J. H., et al., 1997. Sand Source of Sand Dune and Modern Desertification Process in Jiandang Wide Valley Area of Yarlung Zangbo River. *Journal of Desert Research*, 17(4): 377–382 (in Chinese with English Abstract).

Liu, Y., Wang, Y. S., Shen, T., 2019. Spatial Distribution and Formation Mechanism of Aeolian Sand in the Middle Reaches of the Yarlung Zangbo River. *Journal of Mountain Science*, 16(9): 1987–2000. https://doi.org/10.1007/s11629-019-5509-5

Lyu, Y. L., Shi, P. J., Han, G. Y., et al., 2020. Desertification Control Practices in China. *Sustainability*, 12(8): 3258. https://doi.org/10.3390/su12083258

Mirzabaev, A., Annagylyjova, J., Amirova, I., 2019. The Aral Sea Basin: Water for Sustainable Development in Central Asia, Chapter: Environmental Degradation. Routledge, London. 66–85. https://doi.org/10.4324/9780429436475

Moghaddam, M. H. R., Sedighi, A., Fasihi, S., et al., 2018. Effect of

Environmental Policies in Combating Aeolian Desertification over Sejzy Plain of Iran. *Aeolian Research*, 35: 19–28. https://doi.org/10.1016/j.aeolia.2018.09.001

Na, R. S., Du, H. B., Na, L., et al., 2019. Spatiotemporal Changes in the Aeolian Desertification of Hulunbuir Grassland and Its Driving Factors in China during 1980–2015. *CATENA*, 182: 104123. https://doi.org/10.1016/j.catena.2019.104123

Rasmussen, K., Fog, B., Madsen, J. E., 2001. Desertification in Reverse? Observations from Northern Burkina Faso. *Global Environmental Change*, 11(4): 271–282. https://doi.org/10.1016/s0959-3780(01)00005-x

Reynolds, J. F., Smith, D. S., Lambin, E. F., et al., 2007. Global Desertification: Building a Science for Dryland Development. *Science*, 316(5826): 847–851. https://doi.org/10.1126/science.1131634

Shen, W. S., Li, H. D., Sun, M., et al., 2012. Dynamics of Aeolian Sandy Land in the Yarlung Zangbo River Basin of Tibet, China from 1975 to 2008. *Global and Planetary Change*, 86/87: 37–44. https://doi.org/10.1016/j.gloplacha.2012.01.012

Shen, W. S., Li, H. D., 2012. Remote-Sensing Monitoring and Ecological Restoration on Aeolian Sandy Land in the Yarlung Zangbo River Basin on the Tibetan Plateau. China Environmental Press, Beijing. 3–12 (in Chinese)

Shen, W. S., Zhao, W., Wang, X. D., et al., 2015. Study on Ecological Carrying Capacity and Sustainable Development in Tibet. China Environmental Press, Beijing. 20–42 (in Chinese)

Shi, X. N., Zhang, F., Lu, X. X., et al., 2018. Spatiotemporal Variations of Suspended Sediment Transport in the Upstream and Midstream of the Yarlung Tsangpo River (the Upper Brahmaputra), China. *Earth Surface Processes and Landforms*, 43(2): 432–443. https://doi.org/10.1002/esp.4258

Wang, F., Pan, X. B., Wang, D. F., et al., 2013. Combating Desertification in China: Past, Present and Future. *Land Use Policy*, 31: 311–313. https://doi.org/10.1016/j.landusepol.2012.07.010

Wang, T., Zhu, Z. D., Wu, W., 2002. Sandy Desertification in the North of China. *Science in China Series D*: *Earth Sciences*, 45(1): 23–34. https://doi.org/10.1007/bf02878385

Wang, X., Chen, F. H., Dong, Z., et al., 2005. Evolution of the Southern Mu US Desert in North China over the Past 50 Years: An Analysis Using Proxies of Human Activity and Climate Parameters. *Land Degradation & Development*, 16(4): 351–366. https://doi.org/10.1002/ldr.663

Wang, X. M., Zhang, C. X., Hasi, E., et al., 2010. Has the Three Norths Forest Shelterbelt Program Solved the Desertification and Dust Storm Problems in Arid and Semiarid China? *Journal of Arid Environments*, 74(1): 13–22. https://doi.org/10.1016/j.jaridenv.2009.08.001

Wang, X. M., Yang, Y., Dong, Z. B., et al., 2009. Responses of Dune Activity and Desertification in China to Global Warming in the Twenty-First Century. *Global and Planetary Change*, 67(3/4): 167–185. https://doi.org/10.1016/j.gloplacha.2009.02.004

Wang, Z. H., Lin, W. L., Ding, R. X., 2018. Quantitative Measurement of Bedding Orientation Using Remote Sensing Data: Yili Basin, Northwest China. *Journal of Earth Science*, 29(3): 689–694. https://doi.org/10.1007/s12583-017-0943-1

Wang, Z. Y., Li, Z. W., Xu, M. Z., et al., 2016. River Morphodynamics and Stream Ecology of the Qinghai-Tibet Plateau. CRC Press/Balkema, Boca Raton. 45–52

Xu, D. Y., Ding, X., 2018. Assessing the Impact of Desertification Dynamics on Regional Ecosystem Service Value in North China from 1981 to 2010. *Ecosystem Services*, 30(A): 172–180. https://doi.org/

10.1016/j.ecoser.2018.03.002

Xu, D. Y., Li, C. L., Song, X., et al., 2014. The Dynamics of Desertification in the Farming-Pastoral Region of North China over the Past 10 Years and Their Relationship to Climate Change and Human Activity. *CATENA*, 123: 11–22. https://doi.org/10.1016/j.catena.2014.07.004

Xu, D. Y., Kang, X. W., Qiu, D. S., et al., 2009. Quantitative Assessment of Desertification Using Landsat Data on a Regional Scale—A Case Study in the Ordos Plateau, China. *Sensors*, 9(3): 1738–1753. https://doi.org/10.3390/s90301738

Xu, Z. W., Lu, H. Y., 2021. Aeolian Environmental Change Studies in the Mu Us Sandy Land, North-Central China: Theory and Recent Progress. *Acta Geographica Sinica*, 76: 1–23. https://doi.org/10.11821/dlxb202109012 (in Chinese with English Abstract)

Xue, W., 2014. Statistical Analysis and SPSS Application. China Renmin University Press, Beijing. 209–260 (in Chinese)

Xue, X., Guo, J., Han, B. S., et al., 2009. The Effect of Climate Warming and Permafrost Thaw on Desertification in the Qinghai-Tibetan Plateau. *Geomorphology*, 108(3/4): 182–190. https://doi.org/10.1016/j.geomorph.2009.01.004

Yang, J. H., Xia, D. S., Gao, F. Y., et al., 2020a. Aeolian Deposits in the Yarlung Zangbo River Basin, Southern Tibetan Plateau: A Brief Review. *Advances in Earth Science*, 35(8): 863–877 (in Chinese with English Abstract)

Yang, J. H., Xia, D. S., Wang, S. Y., et al., 2020b. Near-Surface Wind Environment in the Yarlung Zangbo River Basin, Southern Tibetan Plateau. *Journal of Arid Land*, 12(6): 917–936. https://doi.org/10.1007/s40333-020-0104-8

Yang, M. X., Nelson, F. E., Shiklomanov, N. I., et al., 2010. Permafrost Degradation and Its Environmental Effects on the Tibetan Plateau: A Review of Recent Research. *Earth-Science Reviews*, 103(1/2): 31–44. https://doi.org/10.1016/j.earscirev.2010.07.002

Yang, Y. C., 1984. Aeolian Landform on the Banks of River Valley—Case Study on Yarlung Zangbo River Valley. *Journal of Desert Research*, 4(3): 12–15 (in Chinese with English Abstract)

Yao, T. D., Li, Z. G., Yang, W., et al., 2010. Glacial Distribution and Mass Balance in the Yarlung Zangbo River and Its Influence on Lakes. *Chinese Science Bulletin*, 55(20): 2072–2078. https://doi.org/10.1007/s11434-010-3213-5

Yao, T. D., Piao, S. L., Shen, M. G., et al., 2017. Chained Impacts on Modern Environment of Interaction between Westerlies and Indian Monsoon on Tibetan Plateau. *Bulletin of Chinese Academy of Sciences*, 32(9): 976–984 (in Chinese with English Abstract)

Yao, T. D., Zhu, L. P., 2006. The Response of Environmental Changes on Tibetan Plateau to Global Changes and Adaptation Strategy. *Advances in Earth Science*, 21(5): 459–464 (in Chinese with English Abstract)

Zeng, H. W., Wu, B. F., Zhang, M., et al., 2021. Dryland Ecosystem Dynamic Change and Its Drivers in Mediterranean Region. *Current Opinion in Environmental Sustainability*, 48: 59–67. https://doi.org/10.1016/j.cosust.2020.10.013

Zhao, W. Z., Xiao, H. L., Liu, Z. M., et al., 2005. Soil Degradation and Restoration as Affected by Land Use Change in the Semiarid Bashang Area, Northern China. *CATENA*, 59(2): 173–186. https://doi.org/10.1016/j.catena.2004.06.004

Zhao, Y. B., He, Z. W., Ni, Z. Y., et al., 2012. Spatial Feature of Desertification in Qushui-Naidong Area of Yarlung Zangbo River. *Journal of Arid Land Resources and Environment*, 26(8): 135–140 (in Chinese with English Abstract)

Zhou, N., Zhang, C. L., Wu, X. X., et al., 2014. The Geomorphology and Evolution of Aeolian Landforms within a River Valley in a Semi-Humid Environment: A Case Study from Mainling Valley, Qinghai-Tibet Plateau. *Geomorphology*, 224: 27–38. https://doi.org/10.1016/j.geomorph.2014.07.012

Zhu, Z. D., Chen, G. T., et al., 1994. Sandy Desertification in China. Science Press, Beijing. 217–233 (in Chinese)